MODIFICATION OF HOMESTEAD HOLLOW AT THE INSIGHT LANDING SITE BASED ON THE DISTRIBUTION AND PROPERTIES OF LOCAL DEPOSITS. J. A. Grant[1], N. H. Warner[2], C. M. Weitz[3], M. P. Golombek[4], S. A. Wilson[1], E. Hauber[5], V. Ansan[6], C. Charalambous[7], N. Williams[4], F. Calef[4], T. Pike[7], A. DeMott[2], M. Kopp[2], H. Lethcoe[4], [1]Center for Earth and Planetary Studies, National Air and Space Museum, Smithsonian Institution, 6th at Independence SW, Washington, DC, 20560 (grantj@si.edu), [2]SUNY Geneseo, Department of Geological Sciences, 1 College Circle, Geneseo, NY 14454, [3]Planetary Science Institute, 1700 East Fort Lowell, Tucson, AZ, 85719, [4]Jet Propulsion Laboratory, California Institute of Technology, Pasadena, CA, [5]German Aerospace Center (DLR), Institute of Planetary Research, [6]University of Nantes, Laboratory of Planetary and Geodynamics, [7]Imperial College, London, Department of Electrical and Electronic Engineering.

Introduction: The Interior Exploration using Seismic Investigations, Geodesy, and Heat Transport (InSight) mission landed at 4.502° N, 135.623° E [1] in the northwest corner of a highly degraded ~25 m-diameter impact crater in Elysium Planitia dubbed "Homestead hollow" [2, 3]. Homestead hollow likely formed hundreds of millions of years ago [4, 5] into regolith derived from an underlying Hesperian-aged basaltic plain [6-9] and is one of many small craters in the area [2]: ~8 craters <10 m-diameter are in or near the hollow (Fig. 1).

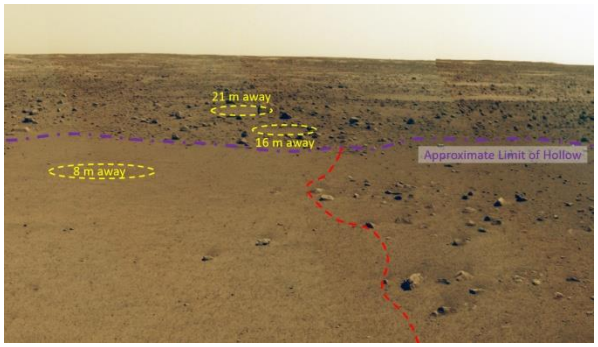

Figure 1. View south across Homestead hollow highlighting the contrast in rock abundance inside versus the margin of the degraded impact structure. Many large rocks along the margin appear perched, whereas some within the hollow are partially buried. The red dashed line distinguishes a higher density of pebbles/cobbles on west/northwest margin of the hollow. Several small impacts (yellow dashed lines) superpose the hollow. A portion of IDC image mosaic D_LRGB_0014_RAS030 100CYL_R__SCIPANQM1.

Description: A HiRISE DEM confirms Homestead hollow is up to ~0.8 m deep [3, 10] and measurements from the DEM and lander images from the Instrument Deployment Camera (IDC) show the interior surface is quite flat down to the cm-scale and slopes <3° to the southeast. The hollow lacks an elevated rim, but the margin does show a significant increase in rocks of cobble up to boulder size as compared to the relatively smooth interior. Many of the rocks along the margin of the hollow are largely to mostly exposed, with many appearing perched the surface. The margin is also devoid of bedforms or other evidence of widespread fines. The lander rockets at least partially cleared surface dust to a range just beyond the hollow interior and produced a radiating pattern of small (<1 cm) debris chutes or ridges separated by grooves more proximal to the lander. Nevertheless, initial mapping using lander images (Fig. 2) shows mostly sand to pebble-sized fines occur across the floor of the hollow [11] that is variably punctuated by mostly gravel/pebbles and cobbles. There are more pebbles and cobbles (>2 cm) on and/or partially embedded on the west/northwest hollow margin (Figs. 1 and 2) [3] where there are ~3X more fragments per m^2 than in front of the lander. Fragment sphericity, or how equant fragments are, can be defined by the square root of the short axis divided by the long axis as measured in 2D [12-13]. For clasts larger than ~1 cm and within ~1 m of the lander, sphericity averages 0.84 (range 0.64-1.0, +/- 0.1). By contrast, average sphericity at the Pathfinder, Gusev, and Gale landing sites is 0.72-0.75 (with a broader range, but similar standard deviation) [13-15] and is also less in most terrestrial environments [14].

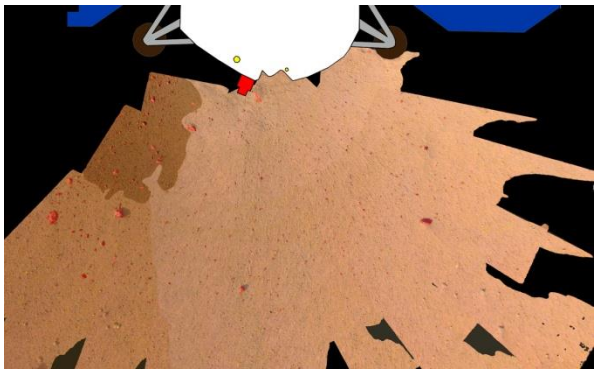

Figure 1. InSight WebGIS [16] composite of lander workspace and vicinity. IDC mosaic F2MMWKSSM1 (2 mm pixel-scale) overlain by Geology Group map of soils and rocks. Medium and dark brown indicate medium coarse sand to cobble unit and coarser sand to pebble unit, respectively. Light brown unit is a finer sand to cobble unit. Rock density is higher in darker brown units. Lander footpad centers ~1.4 m apart. North is up.

Many fragments closer to the lander, especially near the western front footpad, are reddish-brown material, often appear platy and/or sometimes broken in place,

and contrast with darker-gray, sub-angular pebbles observed elsewhere. Pits ~10-20 cm deep were excavated underneath the lander by the landing rockets (Fig. 3) that retain steep walls and reveal possible stratigraphy.

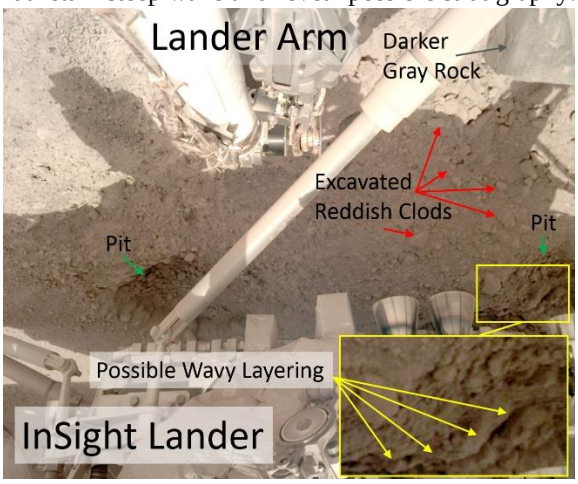

Figure 3. ~10-20 cm deep pits excavated by rocket motors (stretched to highlight shadowed areas). Pit walls reveal indurated materials in possible wavy layers (yellow arrows) and most material was excavated in fairly equant clods that are redder than the darker gray blocks elsewhere (top right). North down, InSight IDC image D000M0014_597774532EDR_F0000_0130M1.

Discussion: The nature and juxtaposition of attributes of Homestead hollow and comparison to similar impact features formed into basaltic rubble in Gusev crater [17-19] enables a first-order evolution to be defined. Based on a diameter of 25 m, Homestead hollow was initially ~3.8 m deep with a ~1 m rim [3, 4]. Early gravity-driven slope processes on the crater wall contributed to infilling and rim modification [3, 4] that slowed as slopes decreased. In addition, local ejecta surfaces initially exposed fines in disequilibrium with the wind regime and/or surface roughness, thereby resulting in deflation and further infilling as fines were transported back into the crater and buried many rocks [17-19]. Eolian stripping of the ejecta results in a rockier-appearing rim with many perched fragments. As early slope-driven and eolian rim modification and infilling slowed, further rim degradation became weathering-limited. Moreover, not all transported sediment returned to the crater, (e.g., bright areas beyond the hollow, Fig. 1) so early infilling was incomplete. Subsequent and ongoing eolian degradation depends on the infrequent production of fines by new impacts and very slow weathering of resistant basaltic rocks and is accompanied by minor mass wasting that together eventually breaks down larger blocks and removes most of the hollow rim.

The persistence of a depression within the hollow after erosion of the rim [3] may reflect a surface in equilibrium with the wind or incomplete infilling due to limited sediment supply. Any ongoing, slow net infilling likely includes ejecta fragments occurring as rocky horizons and delivered during formation of nearby craters. While some fragments on the rockier west/northwest edge of the hollow may protrude infill where it thins at the crater margin [3], others are likely examples of later-arriving ejecta: many are too small to protrude from the ~1 m infill farther from the crater margin [3] and they do not display increasing burial from the margin if they lined the pristine structure. Moreover, others are perched implying more recent emplacement.

Partial burial of some clasts in the hollow (Figs. 1 and 2) and the possible wavy stratigraphy exposed in pits (Fig. 3) relates to a more fine-grained component of later and perhaps ongoing slow infilling. Contributions from slow weathering and transport of material from along the hollow rim is likely augmented by dust and occasional influx of eolian sediments during initial degradation of nearby, later forming craters. The apparent competence of the material (Fig. 3) implies weak induration, perhaps forming a duricrust related to diffusional exchanges of water vapor between the atmosphere and soils [3] as has been observed elsewhere, albeit in lesser thickness [e.g., 20]. Periodic influx of sediments and/or longer and/or cyclical evolution of pedogenic duricrust due to orbital variations may all contribute to the possible wavy stratigraphy and thickness of the sequence (Fig. 3). Excavation produced the reddish clods most numerous by the front-west footpad, roughly equant, and likely contribute to the high sphericity and fragment density in the western workspace (Figs. 2 and 3).

References: [1] Parker, T., et al. (2019), 50th *LPSC*, this meeting, [2] Golombek et al., et al. (2019), 50th *LPSC*, this meeting. [3] Warner et al. (2019) 50th *LPSC*, this meeting. [4] Sweeney, J., et al., (2018), *JGR*, 123, 2732-2759. [5] Wilson, S. A. et al. (2019), 50th *LPSC*, this meeting. [6] Golombek, M., et al., (2017), *SSR*, 211, 5-95. [7] Warner, N.H., et al., (2017), *SSR*, 211, 147-190. [8] Golombek, M., et al., (2018), *SSR*, 214, 84. [9] Tanaka, K., et al., (2014), *U.S. Geol. Surv. Sci. Invest. Map*, 3292. [10] Fergason, R., et al., (2017), *SSR*, 211, 109-133. [11] Weitz et al. (2019), 50th *LPSC*, this meeting. [12] Riley, N.A. (1941), *J. Sed. Petrol*, 11, 94–97. [13] Yingst et al. (2016), *Icarus*, 280, 72-92. [14] Yingst et al. (2007), *JGR*, 112, 0.1029/2005JE002582. [15] Yingst et al. (2008), *JGR*, 113, 10.1029/2008JE003179. [16] Calef et al. (2019), 50th *LPSC*, this meeting. [17] Grant et al. (2004), *Science*, 305, 807-810, 10.1126/science.1099849. [18] Grant et al. (2006), *GRL*, 33, 10.1029/2006GL026964. [19] Grant et al. (2006), *JGR*, 111, 10.1029/2005JE002465. [20] Arvidson et al. (2010), *JGR*, 115, 10.1029/2010JE003633.